Communication

Selective Recognition and Reversible "Turn-Off" Fluorescence Sensing of Acetate (CH₃COO⁻) Anion at Ppb Level Using a Simple Quinizarin Fluorescent Dye

Mannanthara Kunhumon Noushija †, Ananthu Shanmughan †, Binduja Mohan and Sankarasekaran Shanmugaraju *

Department of Chemistry, Indian Institute of Technology Palakkad, Palakkad 678557, Kerala, India
* Correspondence: shanmugam@iitpkd.ac.in
† These authors contributed equally to this work.

Abstract: A simple and cost-effective optical sensing system based on quinizarin fluorescent dye (**QZ**) for the selective and reversible sensing of CH₃COO⁻ anions is reported. The anion binding affinity of **QZ** towards different anions was monitored using electronic absorption and fluorescence emission titration studies in DMSO. The UV-visible absorption spectrum of **QZ** showed a decrease in the intensity of the characteristic absorption peaks at λ = 280, 323, and 475 nm, while a new peak appeared at λ = 586 nm after the addition of CH₃COO⁻ anions. Similarly, the initial strong emission intensity of **QZ** was attenuated following titration with CH₃COO⁻ anions. Notably, similar titration using other anions, such as F⁻, Cl⁻, I⁻, NO₃⁻, NO₂⁻,′ and H₂PO₄⁻, caused no observable changes in both absorption and emission spectra. The selective sensing of CH₃COO⁻ anions was also reflected by a sharp visual color change from bright green to faint green under room light. Further, the binding was found to be reversible, and this makes **QZ** a potential optical and colorimetric sensor for selective, reversible, and ppb-level detection of CH₃COO⁻ anions in a DMSO medium.

Keywords: chemosensor; fluorescent sensors for anions; quinizarin dye; acetate anion sensing

1. Introduction

The recognition and sensing of anions have gained immense research interest in recent years because of their vital role in various biological, environmental, and industrial processes [1]. For instance, fluoride (F⁻) ions are important for maintaining dental health and treating osteoporosis [2,3], sulphite (SO₃²⁻) ions are used in the preservation industry [4], and CH₃COO⁻ ions play a crucial role in various enzymatic and antibody functions [5]. Superoxide (O₂⁻) ions, which are reactive oxygen species (ROS), exhibit distinctive activity in cell growth and metabolism [6,7]. Phosphate (PO₄³⁻) and halide (X⁻) anions are involved in the activity of enzymes, synthesis of protein, hormone transport, and DNA regulation [8–11]. Cyanide (CN⁻) ions are frequently employed in metallurgy, electroplating, gold mining, resins, herbicides, and the manufacture of various organic chemicals [12]. Although anions are ubiquitous species and play numerous indispensable roles, overexposure to anions can cause severe disorders and be harmful to the environment [13]. Therefore, the qualitative and quantitative detection of anions is of paramount interest.

Among various anions, the CH₃COO⁻ anion in particular has drawn special research focus because of its unique role in biochemical, environmental, and medicinal sciences. It has been a common practice to use the rate of CH₃COO⁻ generation and oxidation as a gauge for the decomposition of organic materials in marine sediments [14] and the trans-metalation of tetrapyrroles [15,16]. The regulation of DNA, hormone transfer, protein synthesis, and enzyme activities are influenced by the recognition of CH₃COO⁻ ions [8–11]. Considering the vitality of CH₃COO⁻ ions in both biological and environmental aspects,

developing suitable sensor systems for the selective, sensitive detection and quantification of CH_3COO^- is an important topic of research. Designing colorimetric and fluorescent anion sensors is of great importance in the current scenario due to their simple procedure, low cost, high sensitivity, and low detection limit [17,18]. In the recent past, several small-molecule-based chemosensors have been developed and successfully employed for selective anion recognition and sensing [19–36]. For the detection of anions, the most prevalent chemosensors are polar -NH protons of urea [37] or thiourea [38], amide [39], pyrrole [40], and imidazolium [41,42] moieties. Among the different non-covalent interactions studied, hydrogen-bonding interactions are particularly beneficial and successful in the interaction of anions with a sensor. Coordinative interactions have also been extensively reported by sensors using metal ions. Sensors that use hydroxyl (-OH) groups as hydrogen bond donors have been explored to a lesser extent, although they can form effective hydrogen bonds with anions or induce deprotonation on anion coordination [43,44].

Anthraquinones are an important class of organic small-molecule fluorescent dyes that have been used extensively for the selective detection of anions, cations, and toxic small molecules [45,46]. Anthraquinone derivatives are substances of substantial chemical and biological interest. For many years, the chromophoric system of anthraquinones has been widely utilized to make textile dyes [47]. In addition, these compounds play a significant role as a class of biologically relevant and pharmaceutically active chromophores as well as an analytical tool for metal sensing [46,48,49]. Quinizarin (**QZ**, 1,4-dihydroxy-anthraquinone) is one type of fluorescent anthraquinone with two hydroxyl groups (See Figure 1 for structure). In this report, we were interested in examining the use of structurally simple **QZ** as a selective and reversible fluorescent sensor for anions. We anticipated that the presence of two -OH groups could act as receptor sites for anion recognition, either through hydrogen-bonding interactions or deprotonation of phenolic-OH protons following the binding of anions that subsequently perturbs the optical properties of the **QZ** sensor. Indeed, electronic absorption and fluorescence titration studies showed that **QZ** can selectively bind with CH_3COO^- anions via a fluorescence quenching-based sensing mechanism. The initial fluorescence emission of **QZ** in DMSO was quenched following the addition of CH_3COO^- anions. Notably, similar fluorescence titration studies using other anions, such as F^-, Cl^-, I^-, NO_3^-, NO_2^-, and $H_2PO_4^-$, exhibited negligible binding affinity with **QZ**. Therefore, **QZ** dye could be a potential optical sensor for the selective and reversible sensing of CH_3COO^- anions.
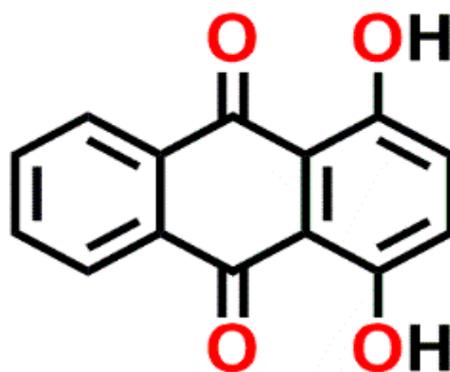
Figure 1. Structure of Quinizarin (**QZ**) fluorescent dye.

2. Materials and Methods

2.1. Materials

The reagents and chemicals were obtained from various commercial sources and used as received, without further purification. For the titration experiments, all anions were added either as tetrabutyl ammonium or sodium salts. The sensor Quinizarin is commercially available and was purchased from Sigma-Aldrich (Bangalore, India) and

used as received. The solvents used for spectroscopic studies were purchased from various suppliers and were HPLC grade.

2.2. Instrumentations

The UV–visible absorption spectra were measured in quartz cuvettes using Thermo Scientific evolution 201 (Waltham, MA, USA) spectrometers. Baseline corrections were applied to all measurements. The fluorescence emission spectra were recorded using the Perkin Elmer-6500 (Waltham, MA, USA) Fluorimeter. All measurements were carried out at 298 K, and spectral data were processed using OriginPro 8.5 (Waltham, MA, USA).

2.3. Fluorescence Sensing Studies

For the titration studies, stock solutions of the **QZ** sensor (1 mM) and different anions (1 mM) as sodium salts, specifically F^-, NO_3^-, and NO_2^-, or tetrabutyl ammonium salts, specifically CH_3COO^-, Cl^-, I^-, and $H_2PO_4^-$, were freshly prepared in DMSO. In a cuvette, 200 μL of 1 mM DMSO solution of **QZ** was taken and diluted with 1800 μL of fresh DMSO solvent. CH_3COO^-, F^-, Cl^-, I^-, NO_3^-, NO_2^-, and $H_2PO_4^-$ salts were added to this solution separately in increments of 20 μL to obtain concentrations up to 90.9 μM. The fluorescence emission intensity of **QZ** was monitored before and after the addition of different anions at various concentrations. For each fluorescence titration experiment, the sample was excited at λ = 437 nm and the fluorescence quenching efficiency was calculated using Equation (1):

$$\text{Quenching efficiency (\%)} = (I_0 - I)/I_0 \times 100 \tag{1}$$

where I_0 is the initial emission intensity of **QZ** in DMSO and I is the intensity after the addition of the anions. The Stern–Volmer quenching constant (K_{SV}) was obtained by fitting the data using the following Stern–Volmer Equation (2):

$$I_0/I = K_{SV}[Q] + 1 \tag{2}$$

K_{SV} was calculated from the slope of the linear curve of the relative changes in emission intensity (I_0/I) vs. the concentration [Q] of CH_3COO^- ions.

3. Results and Discussion

3.1. Anion Sensing Studies Using UV–Vis Titrations

At first, the anion-binding properties of **QZ** were investigated by UV–Vis absorption studies at 25 °C. Titrations were carried out using 1 mM solutions of **QZ** in the DMSO solution. The absorption spectra of **QZ** were recorded before and after the incremental addition (0.0 to 90.9 μM) of the standard solution (1 mM) of different anions: CH_3COO^-, F^-, Cl^-, I^-, $H_2PO_4^-$, NO_2^-, and NO_3^-. As shown in Figure 2A, the DMSO solution of **QZ** (10 μM) exhibited typical anthraquinone characteristic absorption bands: a high-energy band at λ = 280 nm ($\varepsilon = 1.2 \times 10^4$ M^{-1} cm^{-1}), a shoulder band at λ = 323 nm ($\varepsilon = 3.5 \times 10^3$ M^{-1} cm^{-1}), and a low-energy broad peak centered at λ = 475 nm ($\varepsilon = 9.6 \times 10^3$ M^{-1} cm^{-1}). After the addition of 10 equiv. of CH_3COO^- ions, the electronic absorption intensity of the bands at λ = 280 nm and 475 nm decreased significantly, which was accompanied by the appearance of a longer wavelength with a new absorption band at λ = 586 nm corresponding to the complex formation between **QZ** and CH_3COO^- anions (Figure 2A). Notably, the appearance of a clear isosbestic point at λ = 525 nm was consistent with an equilibrium existence of complexed and free **QZ** with CH_3COO^- anions in the DMSO solution (Figure 2C). The significant changes in absorption intensity of **QZ** after the addition of CH_3COO^- anions were also reflected by a sharp visual color change from bright green to faint green under room light before and after the mixing of **QZ** with CH_3COO^- anions (Figure 2A). Interestingly, similar absorption titration studies using 10 equiv. of other competing anions, such as F^-, Cl^-, I^-, NO_3^-, NO_2^-, and $H_2PO_4^-$, showed only little changes in the absorption spectra of **QZ**, and these results demonstrate

that **QZ** can discriminatively and selectively bind with CH_3COO^- anions (Figure 2B). From the electronic absorption titration profile, a perfect linear plot of $1/\Delta A$ vs. $1/[CH_3COO^-]$ was obtained using the Benesi–Hildebrand equation and from the slope of this linear plot; moreover, the association constant K_a for CH_3COO^- ion binding was determined to be 7.63×10^3 M^{-1}, which is comparable to already reported different optical sensors for CH_3COO^- ions (Figure 2D) [26,35,50]. The high value of K_a indicates the strong binding affinity of **QZ** for CH_3COO^- anions in the DMSO solution.
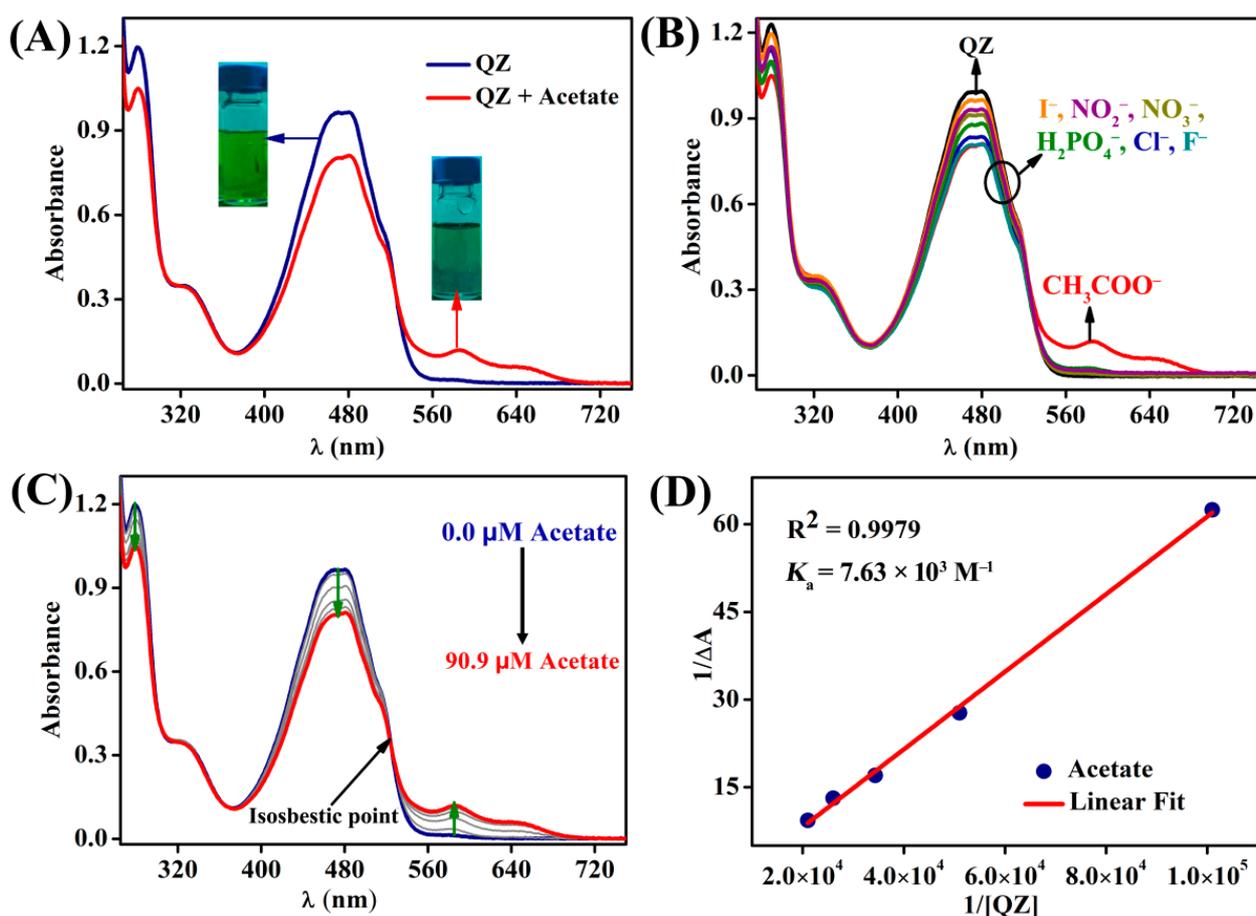
Figure 2. (**A**) The UV–visible absorption spectrum of **QZ** before and after the addition of 10 equiv. of CH_3COO^- anions (Inset: corresponding visual color changes). (**B**) The observed changes in absorption intensity of **QZ** after the addition of 10 equiv. of different anions. (**C**) Relative changes in UV–visible absorption intensity after increasing CH_3COO^- anion concentrations. (**D**) Corresponding Benesi–Hildebrand plot.

3.2. Anion Sensing Using Fluorescence Titrations Studies

The anion-binding propensity of **QZ** was further monitored using fluorescence titration studies in the DMSO solution. The **QZ** sensor was highly emissive due to the presence of emissive anthraquinone moiety and exhibited a broad emission band maximum at $\lambda = 562$ nm, which was quenched drastically after the addition of increasing concentrations of CH3COO$^-$ anions (0.0 to 10 equiv.) (Figure 3C). The observed attenuation in emission intensity after the anion addition was presumably due to the deprotonation of the phenolic-OH group of **QZ** following CH_3COO^- interactions. This binding facilitates the photoinduced electron transfer (PET) from O to π^* orbitals of anthraquinone moiety that results in the subsequent quenching of the fluorescence emission intensity (Scheme 1).
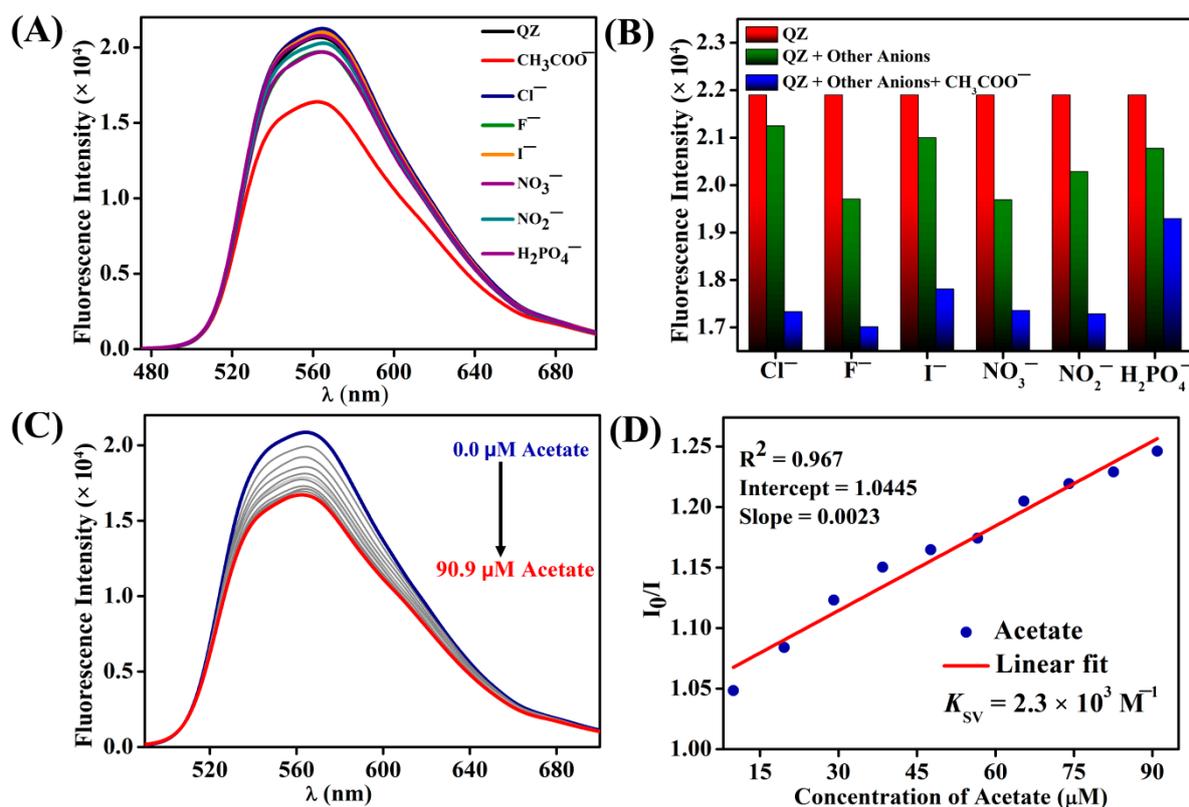
Figure 3. (**A**) The changes in fluorescence emission intensity of **QZ** (10 μM) after the addition of different anions (90.9 μM). (**B**) The competitive binding ability of **QZ** towards CH_3COO^- ions in the co-existence of other anions. (**C**) The relative changes in emission intensity of **QZ** after increasing the concentration of CH_3COO^-. (**D**) Corresponding Stern–Volmer plot.
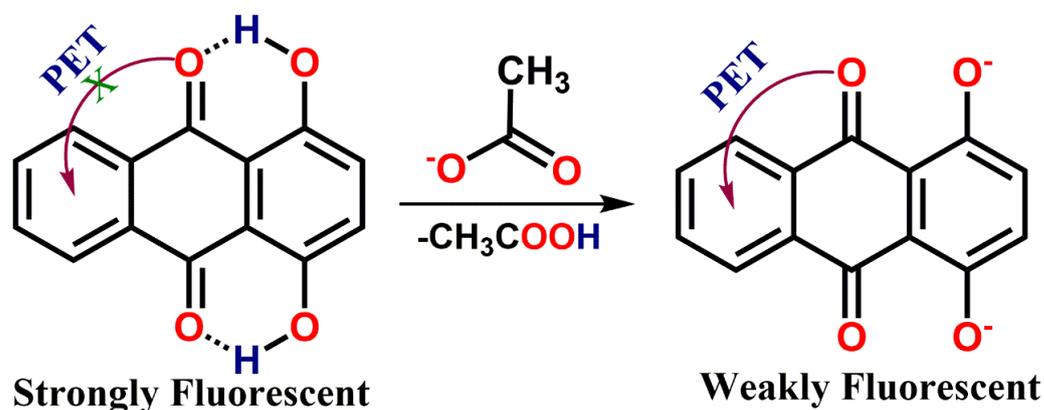
Scheme 1. Proposed fluorescence quenching-based detection of CH_3COO^- through anion-induced deprotonation of OH groups in **QZ**.

The proposed sensing mechanism of anion-induced deprotonation of phenolic-OH groups of **QZ** following CH_3COO^- anion addition was further validated by pH-dependent fluorescence titration studies in the DMSO solution. The fluorescence emission intensity of **QZ** was checked under different pH levels from 3.5 to 11.5. As given in Figure S1, the obtained results revealed that **QZ** is strongly emissive under acidic pH less than 5, and the fluorescence emission intensity was found to decrease under basic pH up to 7. With further increases in pH from 10 to 11.5, **QZ** was almost poorly emissive, presumably due to the deprotonation of phenolic-OH groups under basic pH, which resulted in significant fluorescence quenching of **QZ** due to the proposed PET transition from O to π* orbitals of anthraquinone. We further performed computational calculations to probe the cyclic

stability of **QZ** and support the proposed PET transition. The energy-minimized structure of **QZ** verified that the proposed hydrogen-bonded cyclic structure is feasible and stable (see Figure S2). Moreover, the highest-occupied molecular orbital (HOMO) of deprotonated **QZ^{2-}** was higher in energy than the lowest-unoccupied molecular orbital (LUMO) of the **QZ** sensor, which confirms that the existence of the PET transition from O to π* orbitals of anthraquinone causes the observed fluorescence quenching. A perfectly linear Stern–Volmer plot was obtained from the fluorescence titration data, and the calculated Stern–Volmer quenching constant was found to be $K_{SV} = 2.3 \times 10^3$ M^{-1}. The high value of K_{SV}, again, confirms the strong binding affinity of **QZ** for CH$_3$COO$^-$ anions (Figure 3D).

To establish the sensing selectivity of **QZ** towards CH$_3$COO$^-$ ions, we performed similar fluorescence titration studies using other competing anions, such as F$^-$, Cl$^-$, I$^-$, H$_2$PO$_4^-$, NO$_2^-$, and NO$_3^-$. As depicted in Figure 3A, only CH$_3$COO$^-$ anions elicited significant fluorescence quenching with no other spectral changes seen, whereas F$^-$, Cl$^-$, I$^-$, NO$_2^-$, and NO$_3^-$ anions showed almost negligible fluorescence quenching effects. Thus, **QZ** can be a selective "turn-off" fluorescent sensor for CH$_3$COO$^-$ anions. To further corroborate the high selectivity, we carried out competitive fluorescence sensing studies on other anions under the same experimental conditions. As shown in Figure 3B, the initial fluorescence emission intensity (red bar) of **QZ** did not change (green bar) significantly after the addition of different anions, such as F$^-$, Cl$^-$, I$^-$, H$_2$PO$_4^-$, NO$_2^-$, and NO$_3^-$. However, the subsequent mixing of CH$_3$COO$^-$ anions exhibited a dramatic fluorescence quenching (blue bar). These results further validated the high selectivity of **QZ** for CH$_3$COO$^-$ anion detection. It is worth mentioning that in the presence of H$_2$PO$_4^-$, CH$_3$COO$^-$ anions showed a moderate fluorescence quenching effect, which may be due to the possible interference from H$_2$PO$_4^-$ anions because of their similar basicity and charge density with CH$_3$COO$^-$ anions [50].

Gratifyingly, the observed selective sensing of CH$_3$COO$^-$ anions was also clearly visible to the naked eye. As shown in Figure 4A, the initial bright-orange color of **QZ** changed to colorless after adding CH$_3$COO$^-$ anions under UV light irradiation, and a bright green solution changed to faint green under room light. However, no visible color changes were observed for **QZ** in presence of other anions; thus, the fluorescent dye **QZ** can be used as a colorimetric probe for CH$_3$COO$^-$ ion detection. Moreover, we fabricated a filter paper-based colorimetric sensor for the detection of CH$_3$COO$^-$ ions. As depicted in Figure 4B, the initial green emission of drop-casted **QZ** on filter paper changed to non-fluorescent after mixing a drop of the CH$_3$COO$^-$ solution; thus, **QZ** can be realized as a suitable sensor for the detection of CH$_3$COO$^-$ anions both in solution and solid phases.
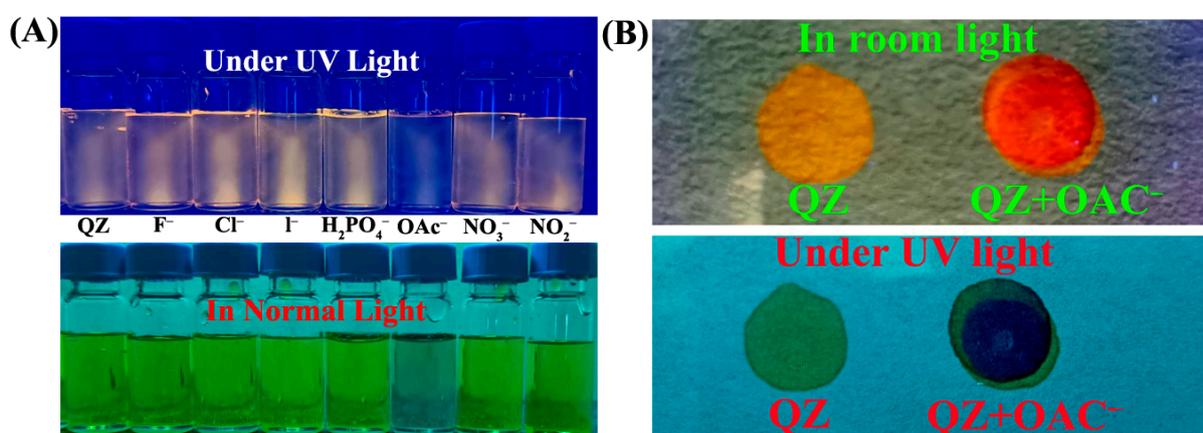
Figure 4. (**A**) The observed visual color changes for **QZ** in DMSO solution after the addition of different anions. (**B**) The color changes observed for **QZ** coated on filter paper before and after the mixing of CH$_3$COO$^-$ anions.

To meet the practical uses, the sensor must be reversible and fluorescence sensing properties should be regenerable. To verify this, we carried out a fluorescence titration experiment employing the polar solvent H_2O as a potential competing solvent to establish the reversibility of **QZ** for CH_3COO^- sensing. As seen in Figure 5A, the addition of H_2O can effectively protonate O^- to form back the original OH groups, thereby leading to the recovery of emission intensity of unbound **QZ** dye. The sensitivity of **QZ** was additionally determined from the plot of changes in emission intensity as a function of CH_3COO^- anions at minute concentrations (Figure 5B). From the plot, the limit of detection (LoD) was determined to be 38 ppb, which is quite low for the detection of CH_3COO^- ions prevalent in many chemical and biological systems.
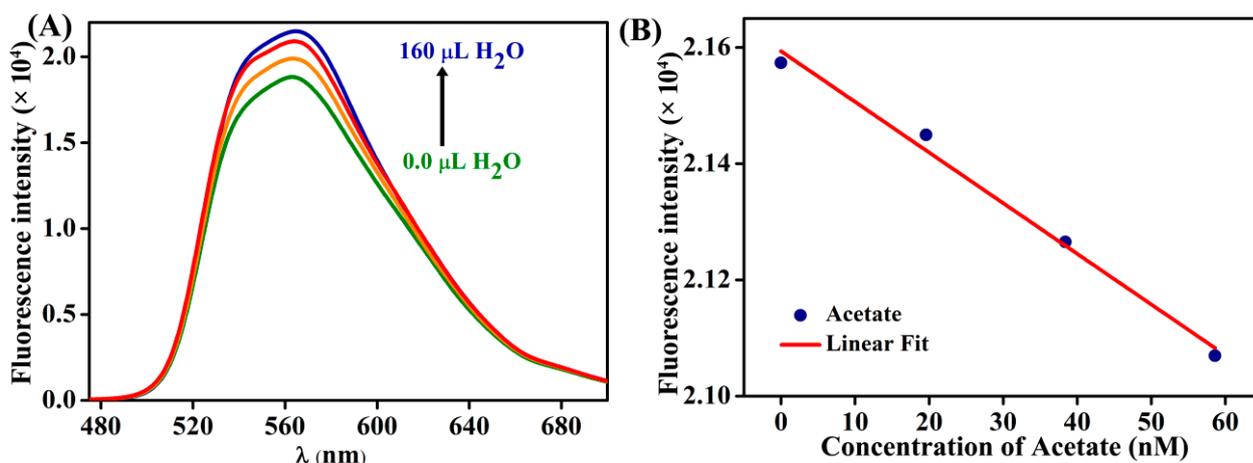
Figure 5. (**A**) Regeneration of fluorescence emission of **QZ** following titration with H_2O at 25 °C. (**B**) The sensitivity plot indicates that the limit of detection is at the ppb level.

4. Conclusions

In conclusion, we have presented a simple quinizarin (**QZ**)-based small-molecule optical sensor for the selective and reversible sensing CH_3COO^- anions in DMSO. Electronic absorption and fluorescence titration studies demonstrated that the **QZ** sensor could selectively recognize CH_3COO^- in presence of various other competing anions (F^-, Cl^-, I^-, NO_3^-, NO_2^-, and $H_2PO_4^-$). The initial emission intensity of **QZ** was remarkably quenched upon the addition of CH_3COO^- ions, which was attributed to the deprotonation of phenolic -OH groups of **QZ** following CH_3COO^- anion addition. Moreover, the observed selective binding of CH_3COO^- anions was also reflected by sharp visual color changes both in solution and solid phases. In summary, the CH_3COO^- anion sensing properties of the fluorescent dye **QZ** are comparable to several reported small-molecule-based fluorescent sensors (see Table S1); hence, **QZ** can be a possible optical and colorimetric sensor for the detection and quantification of CH_3COO^- anions. Further work is in progress to functionalize **QZ** to make it a practically feasible water-soluble sensor for its application in the chemosensing of biologically relevant and environmentally concerned analytes.

References

1. Goshisht, M.K.; Tripathi, N. Fluorescence-based Sensors as an Emerging Tool for Anion Detection: Mechanism, Sensory materials, and Applications. *J. Mater. Chem. C* **2021**, *9*, 9820–9850. [CrossRef]
2. Pal, A.; Karmakar, M.; Bhatta, S.R.; Thakur, A. A Detailed Insight into Anion Sensing based on Intramolecular Charge Transfer (ICT) Mechanism: A Comprehensive Review of the Years 2016 to 2021. *Coord. Chem. Rev.* **2021**, *448*, 214167. [CrossRef]
3. Ali, R.; Razi, S.S.; Gupta, R.C.; Dwivedi, S.K.; Misra, A. An Efficient ICT-based Fluorescent Turn-on Dyad for Selective Detection of Fluoride and Carbon dioxide. *New J. Chem.* **2016**, *40*, 162–170. [CrossRef]
4. De Azevedo, L.C.; Reis, M.M.; Motta, L.F.; da Rocha, G.O.; Silva, L.A.; de Andrade, J.B. Evaluation of the Formation and Stability of Hydroxyalkylsulfonic Acids in Wines. *J. Agric. Food Chem.* **2007**, *55*, 8670–8680. [CrossRef] [PubMed]
5. Liu, X.; Cooper, D.E.; Cluntun, A.A.; Warmoes, M.O.; Zhao, S.; Reid, M.A.; Liu, J.; Lund, P.J.; Lopes, M.; Garcia, B.A. Acetate Production from Glucose and Coupling to Mitochondrial Metabolism in Mammals. *Cell* **2018**, *175*, 502–513. [CrossRef] [PubMed]
6. Hayyan, M.; Hashim, M.A.; AlNashef, I.M. Superoxide Ion: Generation and Chemical Implications. *Chem. Rev.* **2016**, *116*, 3029–3085. [CrossRef] [PubMed]
7. Sauer, H.; Wartenberg, M.; Hescheler, J. Reactive Oxygen Species as Intracellular Messengers during Cell Growth and Differentiation. *Cell. Physiol. Biochem.* **2001**, *11*, 173–186. [CrossRef]
8. Bowman-James, K.; Bianchi, A.; García-España, E. *Anion Coordination Chemistry*; John Wiley & Sons: Hoboken, NJ, USA, 2012; ISBN 3527639519.
9. De Silva, A.P.; Gunaratne, H.Q.N.; Gunnlaugsson, T.; Huxley, A.J.M.; McCoy, C.P.; Rademacher, J.T.; Rice, T.E. Signaling Recognition Events with Fluorescent Sensors and Switches. *Chem. Rev.* **1997**, *97*, 1515–1566. [CrossRef] [PubMed]
10. Beer, P.D.; Gale, P.A. Anion Recognition and Sensing: The State of the Art and Future Perspectives. *Angew. Chem. Int. Ed.* **2001**, *40*, 486–516. [CrossRef]
11. Martinez-Manez, R.; Sancenon, F. Fluorogenic, and Chromogenic Chemosensors and Reagents for Anions. *Chem. Rev.* **2003**, *103*, 4419–4476. [CrossRef]
12. Xu, Z.; Chen, X.; Kim, H.N.; Yoon, J. Sensors for the Optical Detection of Cyanide Ion. *Chem. Soc. Rev.* **2010**, *39*, 127–137. [CrossRef] [PubMed]
13. Sun, X.; Wang, Y.; Zhang, X.; Zhang, S.; Zhang, Z. A New Coumarin Based Chromo-Fluorogenic Probe for Selective Recognition of Cyanide Ions in an Aqueous Medium. *RSC Adv.* **2015**, *5*, 96905–96910. [CrossRef]
14. Ho, T.Y.; Scranton, M.I.; Taylor, G.T.; Varela, R.; Thunell, R.C.; Muller-Karger, F. Acetate Cycling in the Water Column of the Cariaco Basin: Seasonal and Vertical Variability and Implication for Carbon Cycling. *Limnol. Oceanogr.* **2002**, *47*, 1119–1128. [CrossRef]
15. Orzeł, Ł.; Fiedor, L.; Wolak, M.; Kania, A.; van Eldik, R.; Stochel, G. Interplay between Acetate Ions, Peripheral Groups, and Reactivity of the Core Nitrogens in Transmetalation of Tetrapyrroles. *Chem. Eur. J.* **2008**, *14*, 9419–9430. [CrossRef] [PubMed]
16. Caltagirone, C.; Gale, P.A. Anion Receptor Chemistry: Highlights from 2007. *Chem. Soc. Rev.* **2009**, *38*, 520–563. [CrossRef] [PubMed]
17. Williams, D.H.; Cox, J.P.L.; Doig, A.J.; Gardner, M.; Gerhard, U.; Kaye, P.T.; Lal, A.R.; Nicholls, I.A.; Salter, C.J.; Mitchell, R.C. Toward the Semiquantitative Estimation of Binding Constants. Guides for Peptide-Peptide Binding in Aqueous Solution. *J. Am. Chem. Soc.* **1991**, *113*, 7020–7030. [CrossRef]
18. Searle, M.S.; Williams, D.H.; Gerhard, U. Partitioning of Free Energy Contributions in the Estimation of Binding Constants: Residual Motions and Consequences for Amide-Amide Hydrogen Bond Strengths. *J. Am. Chem. Soc.* **1992**, *114*, 10697–10704. [CrossRef]
19. Gunnlaugsson, T.; Glynn, M.; Tocci, G.M.; Kruger, P.E.; Pfeffer, F.M. Anion Recognition and Sensing in Organic and Aqueous Media Using Luminescent and Colorimetric Sensors. *Coord. Chem. Rev.* **2006**, *250*, 3094–3117. [CrossRef]
20. Ganjali, M.R.; Hosseini, M.; Hariri, M.; Faridbod, F.; Norouzi, P. Novel Erbium (III)-Selective Fluorimetric Bulk Optode. *Sens. Actuators B Chem.* **2009**, *142*, 90–96. [CrossRef]

21. Sharma, D.; Moirangthem, A.; Sahoo, S.K.; Basu, A.; Roy, S.M.; Pati, R.K.; SK, A.K.; Nandre, J.P.; Patil, U.D. Anion Selective Chromogenic and Fluorogenic Chemosensor and Its Application in Breast Cancer Live Cell Imaging. *RSC Adv.* **2014**, *4*, 41446–41452. [CrossRef]

22. Cametti, M.; Rissanen, K. Highlights on Contemporary Recognition and Sensing of Fluoride Anion in Solution and in the Solid State. *Chem. Soc. Rev.* **2013**, *42*, 2016–2038. [CrossRef] [PubMed]

23. Suksai, C.; Tuntulani, T. Chromogenic Anion Sensors. *Chem. Soc. Rev.* **2003**, *32*, 192–202. [CrossRef] [PubMed]

24. Sharma, D.; Moirangthem, A.; Kumar, R.; Kumar, S.K.A.; Kuwar, A.; Callan, J.F.; Basu, A.; Sahoo, S.K. Pyridoxal-Thiosemicarbazide: Its Anion Sensing Ability and Application in Living Cells Imaging. *RSC Adv.* **2015**, *5*, 50741–50746. [CrossRef]

25. Sharma, D.; Moirangthem, A.; Roy, S.M.; Kumar, A.S.K.; Nandre, J.P.; Patil, U.D.; Basu, A.; Sahoo, S.K. Bioimaging Application of a Novel Anion Selective Chemosensor Derived from Vitamin B$_6$ Cofactor. *J. Photochem. Photobiol. B Biol.* **2015**, *148*, 37–42. [CrossRef] [PubMed]

26. Yadav, U.N.; Pant, P.; Sharma, D.; Sahoo, S.K.; Shankarling, G.S. Quinoline-Based Chemosensor for Fluoride and Acetate: A Combined Experimental and DFT Study. *Sens. Actuators B Chem.* **2014**, *197*, 73–80. [CrossRef]

27. Chandel, M.; Roy, S.M.; Sharma, D.; Sahoo, S.K.; Patel, A.; Kumari, P.; Dhale, R.S.; Ashok, K.S.K.; Nandre, J.P.; Patil, U.D. Anion Recognition Ability of a Novel Azo Dye Derived from 4-Hydroxycoumarin. *J. Lumin.* **2014**, *154*, 515–519. [CrossRef]

28. Tayade, K.; Sahoo, S.K.; Singh, A.; Singh, N.; Mahulikar, P.; Attarde, S.; Kuwar, A. Architecture of Dipodal Ratiometric Motif Showing Discrete Nanomolar Response towards Fluoride Ion. *Sens. Actuators B Chem.* **2014**, *202*, 1333–1337. [CrossRef]

29. Khairnar, N.; Tayade, K.; Bothra, S.; Sahoo, S.K.; Singh, J.; Singh, N.; Bendre, R.; Kuwar, A. Novel Fluorescent Chemosensing of CN− Anions with Nanomolar Detection Using the Zn2+–Isonicotinohydrazide Metal Complex. *RSC Adv.* **2014**, *4*, 41802–41806. [CrossRef]

30. Amendola, V.; Esteban-Gómez, D.; Fabbrizzi, L.; Licchelli, M. What Anions Do to N− H-Containing Receptors. *Acc. Chem. Res.* **2006**, *39*, 343–353. [CrossRef]

31. Ganjali, M.R.; Veismohammadi, B.; Hosseini, M.; Norouzi, P. A New Tb^{3+}-Selective Fluorescent Sensor Based on 2-(5-(Dimethylamino) Naphthalene-1-Ylsulfonyl)-N-Henylhydrazinecarbothioamide. *Spectrochim. Acta Part A Mol. Biomol. Spectrosc.* **2009**, *74*, 575–578. [CrossRef]

32. Martínez-Máñez, R.; Sancenón, F. New Advances in Fluorogenic Anion Chemosensors. *J. Fluoresc.* **2005**, *15*, 267–285. [CrossRef] [PubMed]

33. Gunnlaugsson, T.; Ali, H.D.P.; Glynn, M.; Kruger, P.E.; Hussey, G.M.; Pfeffer, F.M.; dos Santos, C.M.G.; Tierney, J. Fluorescent Photoinduced Electron Transfer (PET) Sensors for Anions; from Design to Potential Application. *J. Fluoresc.* **2005**, *15*, 287–299. [CrossRef] [PubMed]

34. Moragues, M.E.; Martínez-Máñez, R.; Sancenón, F. Chromogenic and Fluorogenic Chemosensors and Reagents for Anions. A Comprehensive Review of the Year 2009. *Chem. Soc. Rev.* **2011**, *40*, 2593–2643. [CrossRef] [PubMed]

35. Sharma, D.; Kumar, S.K.A.; Sahoo, S.K. Vitamin B6 Cofactor Derived Chemosensor for the Selective Colorimetric Detection of Acetate Anions. *Tetrahedron Lett.* **2014**, *55*, 927–930. [CrossRef]

36. Sharma, D.; Sahoo, S.K.; Chaudhary, S.; Bera, R.K.; Callan, J.F. Fluorescence 'Turn-on'Sensor for F− Derived from Vitamin B6 Cofactor. *Analyst* **2013**, *138*, 3646–3650. [CrossRef]

37. Delépine, A.-S.; Tripier, R.; Handel, H. Cyclen-Based Bismacrocycles for Biological Anion Recognition. A Potentiometric and NMR Study of AMP, ADP and ATP Nucleotide Complexation. *Org. Biomol. Chem.* **2008**, *6*, 1743–1750. [CrossRef]

38. Formica, M.; Fusi, V.; Macedi, E.; Paoli, P.; Piersanti, G.; Rossi, P.; Zappia, G.; Orlando, P. New Branched Macrocyclic Ligand and Its Side-Arm, Two Urea-Based Receptors for Anions: Synthesis, Binding Studies, and Crystal Structure. *New J. Chem.* **2008**, *32*, 1204–1214. [CrossRef]

39. Piątek, P.; Kalisiak, J.; Jurczak, J. Synthesis and Chiroptical Properties of Two New Planar-Chiral Macrocycles. *Tetrahedron Lett.* **2004**, *45*, 3309–3311. [CrossRef]

40. Schmuck, C.; Schwegmann, M. A Molecular Flytrap for the Selective Binding of Citrate and Other Tricarboxylates in Water. *J. Am. Chem. Soc.* **2005**, *127*, 3373–3379. [CrossRef]

41. Pfeffer, F.M.; Lim, K.F.; Sedgwick, K.J. Indole as a Scaffold for Anion Recognition. *Org. Biomol. Chem.* **2007**, *5*, 1795–1799. [CrossRef]

42. Fisher, M.G.; Gale, P.A.; Light, M.E. A Simple Benzimidazole-Based Receptor for Barbiturate and Urea Neutral Guests That Functions in Polar Solvent Mixtures. *New J. Chem.* **2007**, *31*, 1583–1584. [CrossRef]

43. Lee, D.H.; Lee, H.Y.; Lee, K.H.; Hong, J.-I. Selective Anion Sensing Based on a Dual-Chromophore Approach. *Chem. Commun.* **2001**, 1188–1189. [CrossRef]

44. Lee, D.H.; Im, J.H.; Son, S.U.; Chung, Y.K.; Hong, J.-I. An Azophenol-Based Chromogenic Pyrophosphate Sensor in Water. *J. Am. Chem. Soc.* **2003**, *125*, 7752–7753. [CrossRef] [PubMed]

45. Liu, Z.; Luo, F.; Chen, T. Phenolphthalein Immobilized Membrane for an Optical PH Sensor. *Anal. Chim. Acta* **2004**, *510*, 189–194. [CrossRef]

46. Hazneci, C.; Ertekin, K.; Yenigul, B.; Cetinkaya, E. Optical PH Sensor Based on Spectral Response of Newly Synthesized Schiff Bases. *Dyes Pigment.* **2004**, *62*, 35–41. [CrossRef]

47. Guari, N.K. Anthraquinone Appended Chemosensors for Fluorescence Monitoring of Anions and/or Metal Ions. *Inorg. Chim. Acta* **2022**, *536*, 120917.

48. Kaur, N.; Kumar, S. Aminoanthraquinone-based Chemosensors: Colorimetric Molecular Logic Mimicking Molecular Trafficking and a Set–Reset Memorized Device. *Dalton Trans.* **2012**, *41*, 5217–5224. [CrossRef] [PubMed]

49. Saini, R.; Kaur, N.; Kumar, S. Quinones-based Molecular Receptors for Recognition of Anions and Metal Ions. *Tetrahedron* **2014**, *70*, 4285–4307. [CrossRef]

50. Shao, J. Quinoline-Based "On-Off" Fluorescent Sensor for Acetate: Effect of Link Mode between Binding Sites and Fluorophore on Fluorescence Changes. *Spectrosc. Lett.* **2012**, *45*, 262–268. [CrossRef]

51. Huang, W.; Lin, H.; Lin, H. Fluorescent Acetate-Sensing in Aqueous Solution. *Sens. Actuators B.* **2011**, *153*, 404–408. [CrossRef]

52. Ghosh, A.; Sengupta, A.; Chattopadhyay, A.; Das, D. A Single Probe for Sensing Both Acetate and Aluminum(III): Visible Region Detection, Red Fluorescence, and Human Breast Cancer Cell Imaging. *RSC Adv.* **2015**, *5*, 24194–24199. [CrossRef]

53. Liu, G.; Shao, J. Selective Ratiometric Fluorescence Detection of Acetate Based on a Novel Schiff Base Derivative. *J. Fluoresc.* **2012**, *22*, 397–401. [CrossRef] [PubMed]

54. Hosseini, M.; Ganjali, M.R.; Veismohammadi, B.; Faridbod, F.; Abkenard, S.D.; Salavati-Niasarie, M. Selective Recognition of Acetate Ion Based on Fluorescence Enhancement Chemosensor. *Luminescence.* **2012**, *27*, 341–345. [CrossRef] [PubMed]

55. Li, Y.; Lin, H.; Cai, Z.; Lin, H. Colorimetric Sensing of Biologically Important Acetate Ion Based on Indole Derivation. *Mini-Rev. Org. Chem.* **2011**, *8*, 25–30. [CrossRef]

56. Zhao, L.Y.; Wang, G.K.; Chen, J.H.; Zhang, L.M.; Liu, B.; Zhang, J.F.; Zhao, Q.H.; Zhou, Y. 1,8-Naphthalimide-based Visible Colorimetric Sensor for the Selective Sensing of Fluoride, Acetate, and Hydroxyl Anions. *J. Fluorine Chem.* **2014**, *158*, 53–59. [CrossRef]

57. Wang, G.; Zheng, T.; Zhang, S.; Ye, J.; Ning, G. Fluorescence Chemosensor for Acetate Ion and Fluorine Ion based on 1,2,4-Triazolyl Substituted Pentaphenylpyridinium. *J. Mol. Struct.* **2021**, *1230*, 129918. [CrossRef]

58. Goswami, S.; Das, A.K.; Aich, K.; Manna, A. Competitive Intra- and Inter-Molecular Proton Transfer in Hydroxynaphthyl Benzothiazole: Selective Ratiometric Sensing of Acetate. *Tetrahedron Lett.* **2013**, *54*, 4215–4220. [CrossRef]

59. Lin, Q.; Liu, X.; Wei, T.B.; Zhang, Y.M. TICT–ICT State Change Mechanism-based Acetate Fluorescent Sensor Act as an "Off–On–Off" Switch and Logic Gate. Sens. *Actuators B.* **2014**, *190*, 459–463. [CrossRef]